Hindawi
Journal of Sensors
Volume 2023, Article ID 7491593, 9 pages
https://doi.org/10.1155/2023/7491593

Research Article

Real-Time Strain Detection Technology for Steel Structures Based on Eddy Current Effect

Shu-an Ji,[1] **Wei-liang Jin**,[2] **Ying Jin**,[2] **Zheng Lin**,[2] **Sen Wang**,[1] **and Qing Li**[1]

[1]*College of Mechanical and Electrical Engineering, China Jiliang University, Hangzhou Zhejiang 310018, China*
[2]*Zhejiang Academy of Special Equipment Science, Hangzhou Zhejiang 310020, China*

Correspondence should be addressed to Qing Li; lqing@cjlu.edu.cn

Received 15 September 2022; Revised 13 November 2022; Accepted 29 December 2022; Published 13 January 2023

Academic Editor: Sangsoon Lim

To avoid strains in steel structures in special equipment caused by excessive alternating loads, which cause stress concentrations in local areas and reduce the strength and pressure-bearing capacity of the steel structures, a method for evaluating the strain state of the steel structures using the eddy current effect is proposed, and the relevant testing device is developed. The RMS voltage and tension values were tested and fitted linearly with sampling time, and their linear correlations after fitting were 0.9978560 and 0.9967905, respectively. To investigate the method's practical application, the effect of strain on the impedance of the eddy current probe was first studied theoretically, followed by the design and fabrication of a strain detection device comprised of an eddy current probe and a signal processing system. Finally, tensile strain experiments were carried out on 5 mm thick standard Q235 steel tensile specimens using a universal tensile machine and the linear equation of RMS voltage versus strain was obtained analytically. Theoretical and experimental tests have shown that the device can detect each strain stage and quantify the strain within the elastic stage by fitting a linear equation.

1. Introduction

Steel structures have numerous applications in modern industry, including amusement rides, pressure vessels, and other special equipment. Its tensile strength and pressure-bearing capacity are crucial as an essential structural material. The strain on the steel structures can significantly impact its strength and pressure-bearing capacity, causing the equipment to fail, and posing a severe safety hazard. For example, steel structures in amusement facilities are prone to large or alternating loads in local areas during operation, resulting in stress concentrations that develop strains and finally cause structural failure. Consequently, the research on strain sensing in steel structures is crucial for special equipment like amusement rides [1]. During strain, steel materials typically exhibit distinct features, such as elastic stage, yield stage, and strengthening stage, the steel structures can be returned to its original state upon unloading during the elastic stage. When the strain of steel material exceeds the elastic stage and continues to load until it reaches the yield limit, the steel structures material begins to fail, and finally necking fracture occurs.

The current state of research on strain detection in steel structures is limited. The use of eddy current effects in detecting special equipment such as large amusement rides is primarily for detecting more apparent defects such as cracks [2]. Traditional strain detection is still in the equipment downtime maintenance of manual detection. The method is time-consuming and labor-intensive and has the disadvantages of low automation, inability to detect in real-time, and high detection errors. And there are also stringent requirements for workers' testing abilities and possibly secondary damage to the steel structure if not done carefully. The conventional resistive strain gauge detection method can be used for online testing, but it requires the strain gauge to be fully coupled to the test site, and the detection range is small and immovable. The detection efficiency is low for work scenarios such as amusement rides, which have an extensive working range and cumbersome component movement trajectories [3].

Based on the analysis presented above, this paper proposes a real-time online detection method for evaluating the strain state of steel structures using the eddy current effect and developing a relevant detection device. The device can be widely used in special equipment composed of steel structures. For example, the bottom stress part of the pressure vessel loading and unloading shall be detected in real-time to prevent damage and leakage of the pressure vessel, and real-time detection of the support structure with a huge instantaneous load such as a roller coaster in the amusement park to prevent the occurrence of safety accidents caused by structural failure. Because the structure of the tested object in this special application scenario is relatively complex, and most of the surfaces are distributed with oil stains, welds, and other factors that affect the test results, compared with the traditional detection system, this method can reasonably use the lift effect to complete a variety of automatic detection methods without contact with the measured object, such as hand-held and automatic scanning. It also has high sensitivity and enables qualitative and quantitative strain analysis by collecting and fitting the induced electrical signals of eddy currents.

2. Strain Detection Principle of Eddy Current Effect

2.1. Principle of Eddy Current Effect. Eddy current inspection is a nondestructive testing method that detects defects in electrically conductive materials. It is based on the theory of electromagnetic induction. Figure 1 depicts the fundamental principles of electromagnetic nondestructive testing.

This paper mainly studies the change of eddy current effect in the process of stress structure and strain of steel structure and reflects the specific state of strain through the induced electrical signal, to prevent sudden failure of steel [4]. When the steel structure is subject to stress and strain, its conductivity and magnetic conductivity will change due to changes in the crystal structure and crystal gap inside the material [5], thus changing the distribution of the eddy current field in the measured conductor, and ultimately leading to the change of the induced electrical signal generated by the eddy current field [6–8]. Therefore, the following theoretical analysis is made on the influence of stress and strain on the induced electrical signal and the conductivity and permeability of the measured conductor:

$$\begin{aligned} \nabla \times \boldsymbol{E} &= -\frac{\partial \boldsymbol{B}}{\partial t}, \\ \nabla \times \boldsymbol{H} &= \boldsymbol{J}, \\ \nabla \cdot \boldsymbol{B} &= 0, \\ \nabla \cdot \boldsymbol{J} &= 0. \end{aligned} \tag{1}$$

According to the analysis of Maxwell equations, the governing equations of the eddy current field can be obtained as Equation (1). Since the excitation signal frequency in this experiment is less than 10 MHz and the electric displacement current is far less than the induced current, the electric displacement current in the ampere loop law can be ignored. Where $\boldsymbol{B}$ is the magnetic induction intensity, $\boldsymbol{E}$ is the electric field intensity, $\boldsymbol{H}$ is the magnetic field intensity, and $\boldsymbol{J}$ is the current density vector.

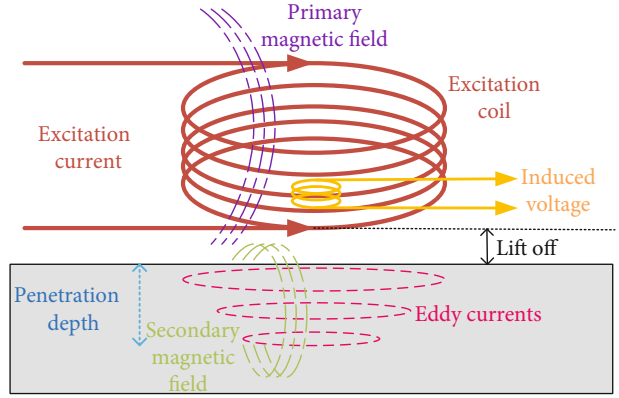

Figure 1: Eddy current testing schematic.

Introducing the magnetic vector potential $\boldsymbol{A}$ that meets $\boldsymbol{B} = \nabla \times \boldsymbol{A}$, the Gauss's law for magnetism is automatically met. Then, the Faraday's law of induction in Equation (1) becomes

$$\nabla \times \left(\boldsymbol{E} + \frac{\partial \boldsymbol{A}}{\partial t} \right) = 0. \tag{2}$$

In addition, the relationship between the scalar potential φ and the electric field strength $\boldsymbol{E}$ is as follows:

$$E = -\frac{\partial A}{\partial t} - \nabla_{\varphi}. \tag{3}$$

For the tested conductor, the electromagnetic constitutive equation satisfies

$$\begin{aligned} \boldsymbol{B} &= \mu \boldsymbol{H}, \\ \boldsymbol{J} &= \gamma \boldsymbol{E}, \end{aligned} \tag{4}$$

where μ and γ are permeability and conductivity, respectively.

This paper deals with the problem of the low-frequency electromagnetic field, and the influence of the electric displacement current can be ignored. Therefore, when the measured conductor is subjected to stress and strain, both μ and γ are functions of stress and strain. In order to simplify the function and have universality, it is assumed that μ and γ can be expressed as functions of equivalent stress and equivalent strain

$$\begin{aligned} \mu &= \mu_0 \mu_r f\left(\sigma_{eq}, \varepsilon_{eq}\right), \\ \gamma &= \gamma_0 g\left(\sigma_{eq}, \varepsilon_{eq}\right), \end{aligned} \tag{5}$$

where f and g are both functions of σ_{eq} and ε_{eq}, σ_{eq} is the equivalent stress, ε_{eq} is the equivalent strain, respectively,

μ_0 is the magnetic permeability in vacuum, μ_r is the initial relative permeability, and γ_0 is the initial conductivity [9].

2.2. Impedance Analysis. The coil's impedance changes as it is subjected to changes in eddy currents. The strain information of the measured object is thus obtained by utilizing the change in the RMS value of the voltage caused by the detection coil's impedance. The transformer model can explain the coupling between an eddy current sensor's detection coil and the measured object [10], as shown in Figure 2.

From the equivalent circuit and Kirchhoff's law, Equation (6) was obtained.

$$\begin{pmatrix} R_1 + j\omega L_1 & -j\omega M \\ -j\omega M & R_2 + j\omega L_2 \end{pmatrix} \begin{pmatrix} I_1 \\ I_2 \end{pmatrix} = \begin{pmatrix} U \\ 0 \end{pmatrix}. \tag{6}$$

In Equation (6), $\omega = 2\pi f$ and the mutual inductance coefficient M between the coil and the test piece is calculated as follows:

$$M = k\sqrt{L_1 L_2}(0 < k < 1). \tag{7}$$

Substituting Equation (7) into Equation (6), Equation (8) was obtained.

$$\begin{aligned} R &= R_1 + \frac{\omega^2 k^2 L_1 L_2}{R_2^2 + (\omega L_2)^2} R_2, \\ L &= L_1 - \frac{\omega^2 k^2 L_1 L_2}{R_2^2 + (\omega L_2)^2} L_2. \end{aligned} \tag{8}$$

In Equation (8), k is denoted as the coupling coefficient, and the magnitude of this value is related to parameters such as the wire diameter of the enameled wire and the structure of the eddy current probe [11]. In this paper, the derivation of Equation (8) validates the feasibility of using the true RMS voltage output from the probe to characterize eddy current changes, and finally the data acquisition and display of the true RMS voltage is used to determine the strain state of the steel structures.

The closed-loop theory as shown in Figure 3.

In practical application, using the closed-loop theory, it is only necessary to calculate the penetration depth in advance [12], and then conduct tensile tests on different steel structure materials to obtain the required characteristic parameters and fitting equations. Finally, the effective value voltage (RMS voltage) collected in the field is substituted into the fitting equation to qualitatively and quantitatively analyze the state parameters of stress and strain.

2.3. Hooke's Law. To quantitatively analyze the strain within the elastic range, this paper proposes to use the generalized Hooke's law [13] to convert the known stress into the strain, to realize the quantitative analysis of the strain within the elastic range. and its formula can be expressed by

$$\frac{F_N}{A} = E\frac{\Delta l}{l}, \tag{9}$$

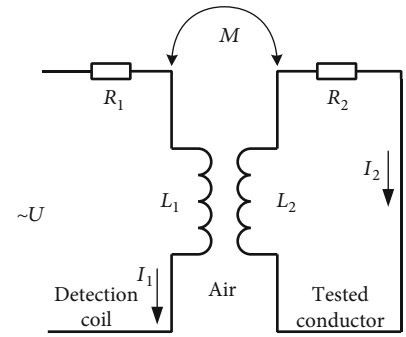

Figure 2: Eddy current sensor equivalent circuit.

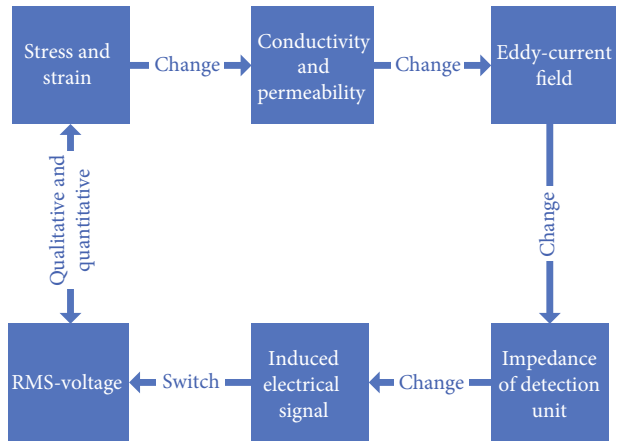

Figure 3: Closed-loop theory.

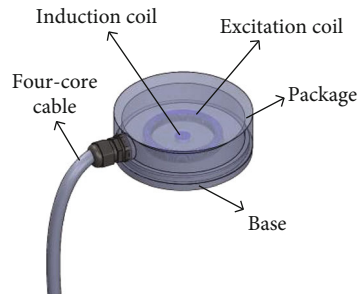

Figure 4: Eddy current probe structure diagram.

$$\sigma = E\varepsilon. \tag{10}$$

In Equation (9), E is the young's modulus of the material, the unit is usually GPa, and E of the same material is a constant; A is the cross-sectional area in mm^2; F is tensile stress in kN; l is the initial length of the test piece, and Δl is the elongation after stress in mm. In Equation (10), σ is the stress and ε is the strain.

When the stress does not exceed the limit state, Equation (10) shows that stress is proportional to strain, and this theory is consistent with the fitting data obtained in the experimental part of this paper. Therefore, the strain experiment of the steel structure can be simulated by the

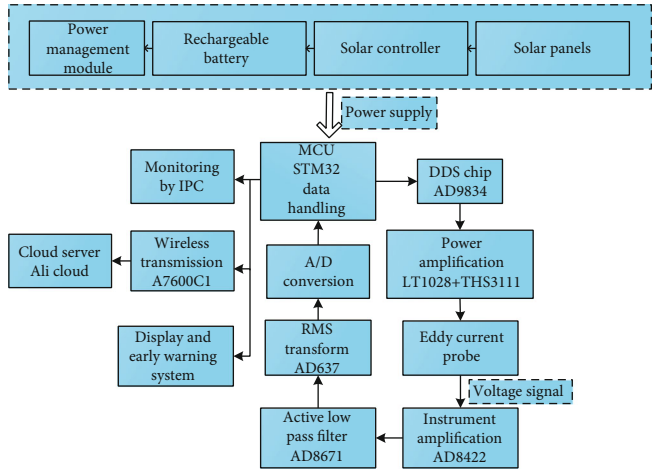

Figure 5: Hardware circuit structure diagram.

tensile experiment of the steel standard specimen, and the strain state can be characterized by the change of eddy current signal caused by the change of stress. Compared with traditional strain measurement, this method can greatly improve the accuracy of quantitative analysis of strain in the elastic range.

3. Eddy Current Probe and Detection System Design

3.1. Eddy Current Probe Design. As an essential part of eddy current detection, the probe's performance directly affects the whole device's sensitivity, so it is important to design and make a suitable eddy current probe. In this paper, the conventional absolute eddy current probe is improved, and a new eddy current probe is designed and manufactured, as shown in Figure 4. The improved probe can respond sensitively to various factors affecting eddy current testing, such as resistivity, magnetic permeability, and geometric shape of the measured material [14]. For defects such as strain, which varies gently and with little difference between adjacent parts of the material, common differential probes are less sensitive to such strain defects and can cause problems such as missed detections [15]. The probe is composed of an excitation unit and a detection unit. The excitation unit can generate a sufficiently large eddy current field in the measured conductor, and the detection unit can sensitively sense the eddy current field changes caused by the strain, thus generating characteristic electrical signals. At the same time, compared with traditional strain detection systems such as resistance strain gauge detection systems, the new probe can complete multiple detection modes to adapt to different application scenarios such as handheld, mobile scanning, and coupling, and any mode will not affect the actual effect of detection. This paper also considers the effect of the lift-off height of the eddy current probe on the detection signal and designs a package housing. The lifting height can be controlled by fitting removable base of different thicknesses to obtain the optimum lifting height when placed. The housing connects the four-core cable to the coil, making it noise-shielded and waterproof.

3.2. Detection System Circuit Design. Figure 5 depicts a circuit diagram of the system for strain detection in steel structures. The system consists of a power supply module, a DDS signal generation module, a power amplification module, an instrumentation amplification module, a filtering module, wireless transmission, and a display and warning module.

The working process of the system is that the STM32 single chip sends frequency output instructions to the DDS chip, and the specified frequency and voltage signals are output through a sine wave generation circuit. Since the peak-to-peak voltage output from the DDS chip is less than 600 mV, which is not enough to excite the excitation coil to produce a relatively strong eddy current, a power amplifier circuit was designed. The power amplifier circuit consists of a two-stage amplifier circuit. In the preceding stage, the LT1028 chip amplifies the amplitude of the sine wave signal by three times. In the latter stage, the THS3111 chip performs power amplification of the sinusoidal signal [16]. The eddy current probe is affected by strain and produces a weak AC voltage signal in millivolts. To prevent the signal from being drowned out by external environments such as noise and temperature, instrumentation amplification, low-pass filtering, and RMS conversion are required. Finally, the analog signal is converted into a digital signal by A/D sampling and transmitted to the microcontroller by SPI serial communication. After processing and analyzing the data, the data is uploaded to AliCloud in real-time through the remote transmission module to complete real-time monitoring tasks such as data display, early warning, and alarm for the upper and lower computers.

In order to meet the requirements for a wide range of detection objects such as special equipment, this system improves the limitation that the traditional eddy current detection system can only complete the task of "one circuit board and one probe". The DDS chip generates multiple sinusoidal signals, which can drive multiple eddy current probes after power amplification, thus completing the array

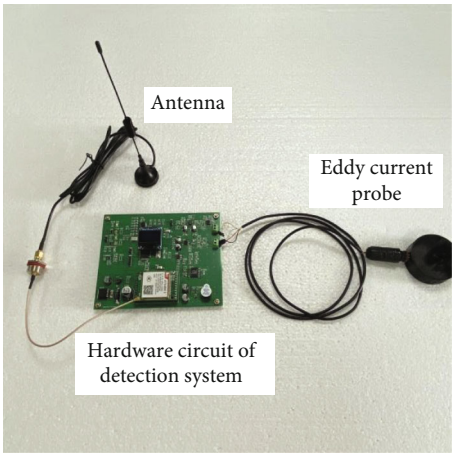

Figure 6: Physical map of detection device.

distribution of multiple sensors and realizing the goal of "one circuit board with multiple probes". At the same time, when the material properties and thickness of the measured object are different, the constant frequency will change the skin depth of the vortex flow field and affect the detection accuracy. For this reason, the system has designed a scanning frequency selection function, to select the most appropriate frequency, and then complete accurate detection. An innovative RMS conversion circuit is added to perform AD-DC conversion of the demodulated electrical signal, On the one hand, the property of RMS conversion circuit makes the conversion result of the detection signal more stable, on the other hand, according to the experiment, it is found that the RMS voltage change law can perfectly correspond to the strain change process described in material mechanics.

Figure 6 depicts the strain detection device for steel structures.

3.3. System Software Design. Figure 7 depicts the flow chart for the system's software component.

After the system is powered on, initialize each module, determine whether the initialization of the MQTT protocol function is successful, and if successful, enter the timing loop function. After entering this cycle, the RMS voltage Vol data is uploaded to Aliyun every A/D sample, and the Vol value is then compared with the experimentally calibrated voltage threshold h at dangerous strain, and if Vol is less than or equal to the threshold, the alarm is turned on. The alarm system is switched off when the key scan recognizes that key KEY1 is pressed. In order to prevent the system program from crashing, the watchdog function is used to restart it if the loop has not been completed within six seconds.

4. Tensile Testing and Data Analysis

4.1. Experimental Platform Construction. In this experiment, a 5 mm thick standard Q235 steel tensile specimen was stretched using a universal tensile machine to simulate the steel structure's tensile strain under the actual working state

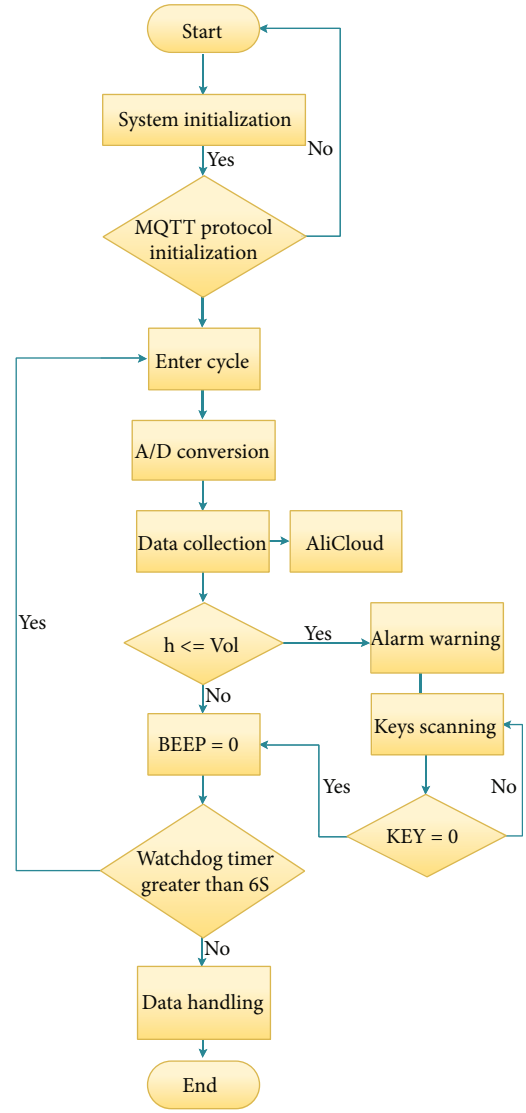

Figure 7: Software program flow chart.

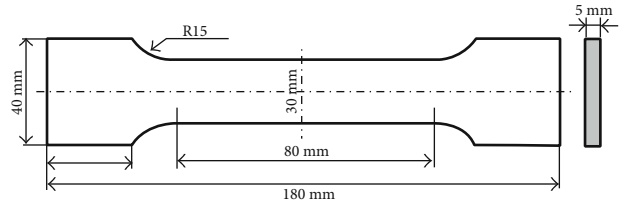

Figure 8: Tensile specimen.

[17–19]. The parametric diagram of this standard tensile specimen is shown in Figure 8.

The eddy current probe is placed in the middle of the tensile specimen and fixed, then the tensile specimen is clamped into the fixture of the universal testing machine, and finally, the PC controls the universal testing machine to complete the loading of the specimen and receive the data in real-time. The detection parts are shown in Figures 9–11.

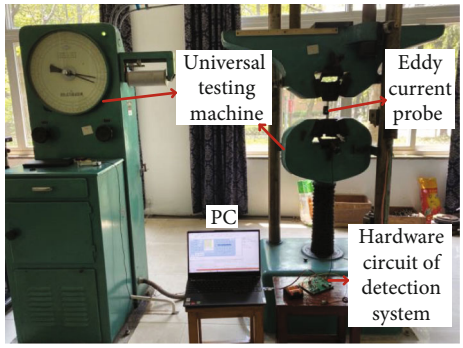

Figure 9: Strain experiment device and equipment.

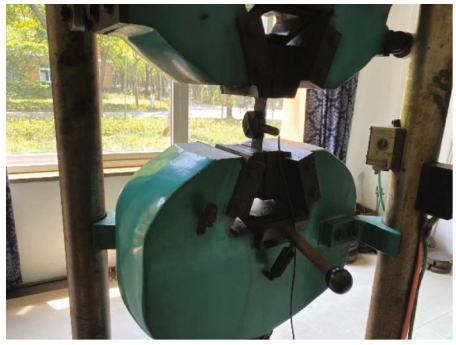

Figure 10: Probe installation and specimen clamping.

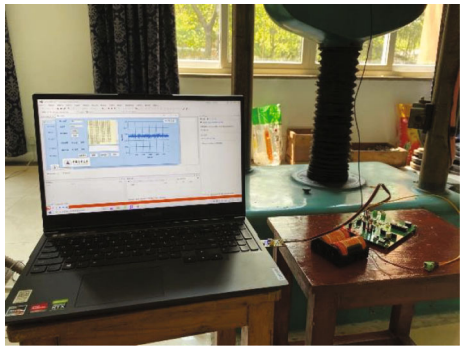

Figure 11: The photo of signalacquisition system.

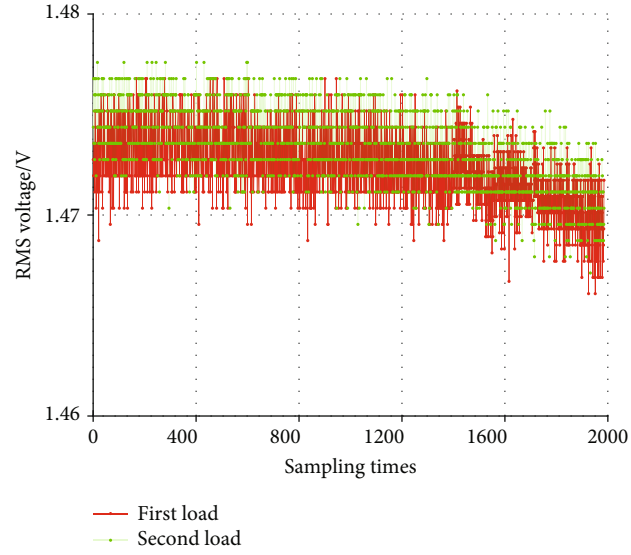

Figure 12: The first part of the experimental data map.

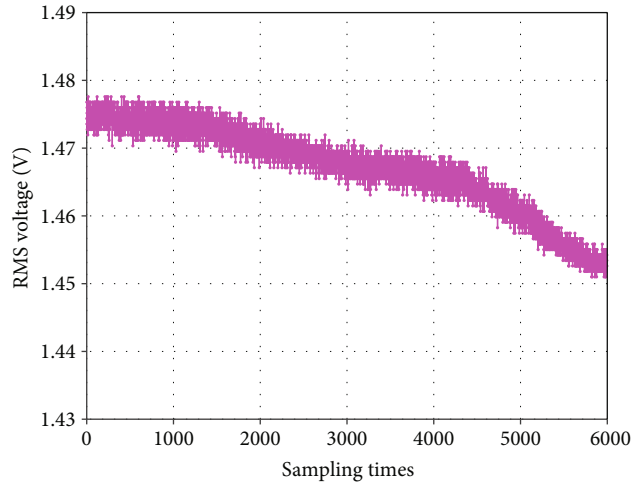

Figure 13: The second part of the experimental data map.

4.2. Experiments and Results. The experiment is divided into the following two parts to verify that the device can accurately and sensitively detect the individual strain states of the steel structures.

Part I: load the steel specimen from 0kN to 18kN for the first time. At this time, the steel specimen is still in the elastic stage. After unloading the load, load the steel specimen with a load of 0kN to 18kN for the second time. Figure 12 shows a graph of the variation in the RMS values of the voltages taken during the two loading experiments.

It can be seen from Figure 12 that in the elastic stage, the RMS value of the initial voltage of the two loads is basically the same, and the changing trend is basically the same. The results show that the device can sensitively detect the elastic properties of steel specimens, this means that if the load is unloaded during the elastic phase, the strain in the steel specimen will return to its initial state.

Part II: Load the steel specimen from 0kN to 40.5kN and maintain the load continuously. Figure 13 shows the change in the RMS voltage collected during load loading.

As can be seen from Figure 13, the changes in the RMS voltage data collected during this experiment can be divided into three stages: smooth, slow decline, and rapid decline. The rate of change of the voltage signal of the steel specimen in the last two stages is more obviously different, and the curve is nearly linear. However, the data curve is not smooth, and the data needs to be filtered to complete the subsequent analysis better.

4.3. Software Filtering and Data Analysis. Due to the short acquisition period set by the microcontroller, the amount

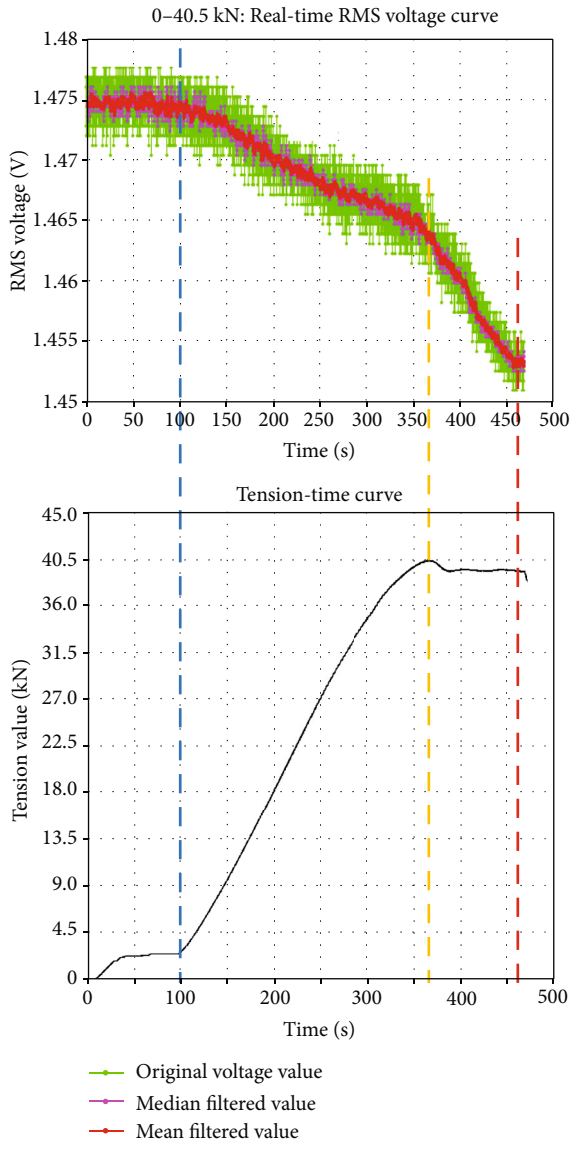

Figure 14: Data comparison diagram.

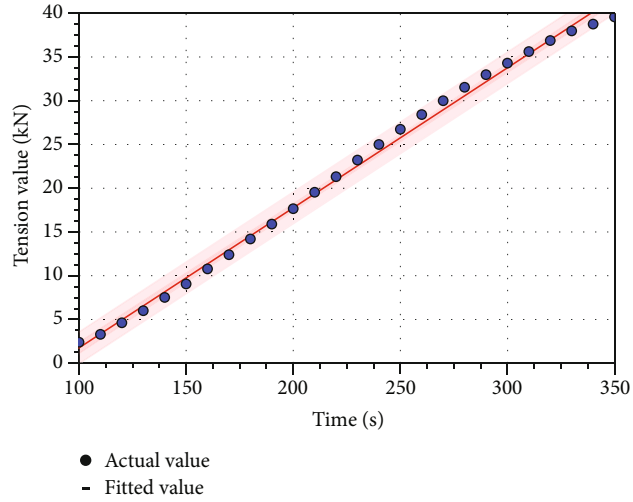

Figure 15: Linear fit plot of tension versus time.

of data collected for the experiment is high, and data fluctuations are caused by a small amount of noise in the signal. As a result, the curve presented by the original data is thick, and curve fitting is difficult, necessitating digital filtering [20]. Median filtering and mean filtering were performed by MATLAB software. A comparative analysis of the filtered data shows that the curve after mean filtering is smoother and the fluctuations in the RMS voltage are smaller, with the interference signal controlled to within 2 mV. The filtered RMS voltage curve better represents the steel specimen's corresponding strain state in the tension change process. The data comparison diagram is shown in Figure 14.

According to the analysis in Figure 14, the value of the RMS voltage remains essentially unchanged after mean filtering in the region 0-100 s in front of the blue dashed line. At this time, the tensile specimen has not yet produced strain. The rising tension is only the clamping fixture clamping specimen necessary to tighten the force, the stage for the clamping stage. The tensile specimen is in the elastic stage in an area of 100-370 s in front of the orange dotted line. The voltage starts to decrease in a nearly linear manner, this phenomenon is consistent with the theory that an increase in the microscopic intercrystalline gap in carbon steel during the elastic phase weakens the eddy current signal. At the same time, the tensile stress increases linearly, so that the strain on the tensile specimen can be calibrated according to Hooke's law using the correspondence between the RMS value of the voltage and the value of the tensile force, thus allowing quantitative testing of it. In front of the red dotted line, that is, in the area of 370-460 s, the rate of change of the RMS value of the voltage increases, while the pull value slowly tends to remain constant after passing the peak value of 40.5kN and remains at around 40.2kN. At this time, the tensile specimen is in the yielding stage. The internal crystal distortion of carbon steel at this stage increases, crystal defects increase, the specimen elongation will increase sharply, and the electrical conductivity decreases, so the rate of change of the voltage RMS at this stage is greater than in the previous stage. After the red dotted line, it enters the strengthening stage, where the test specimen has been destroyed.

4.4. Calibration of Strain in Elastic Stage. In the elastic stage, the fusion filtering algorithm of median filtering and mean filtering is used to smooth the data. Then, the voltage RMS—time and tension value—time curves were fitted using the least squares method. A numerical relationship between the pulling force F_N-t and the RMS voltage Vol-t was obtained, Figures 15 and 16 depict the relationship curves.

The linear fitting equations ($100\,s < t < 350\,s$) can be expressed as

$$F_N = 0.16t - 14.2517,$$
$$Vol = -0.0000354285t + 1.477304. \quad (11)$$

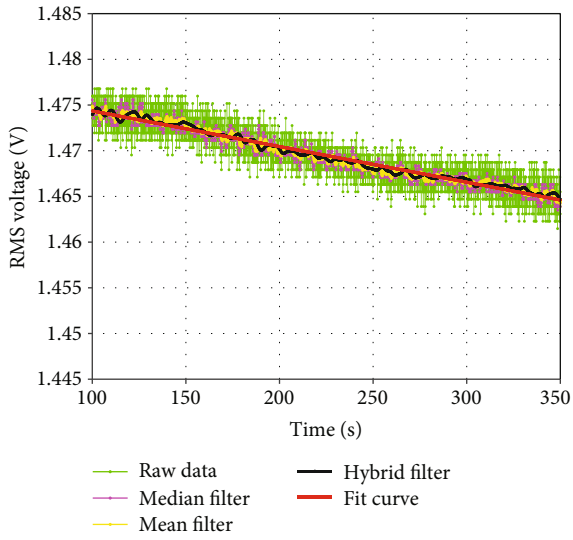

Figure 16: Linear fitting plot of voltage rms versus time.

After fitting, the linear correlation coefficients are 0.9978560 and 0.9967905, which are very close to 1, indicating that the linear equations of tension F_N and voltage RMS value Vol concerning time t have good linear changes. Equation (11) can be used to solve the corresponding relationship between the tension value F_N and the voltage RMS value Vol (take four digits after the decimal point). Units are kN and V, respectively. The linear expression of F_N-Vol can be expressed as

$$F_N = 6657.4572 - 4516.1381 Vol. \quad (12)$$

The Q235 steel used in this experiment has a cross-sectional area A of 150 and Young's modulus E of 196 to 216 GPa, commonly assumed in engineering calculations to be 200 GPa. Substituting the expression for F_N in Equation (12) and the constants E and A into Equation (9). The linear relationship between strain ε and RMS voltage value Vol can be calculated as

$$\varepsilon = 0.2219 - 0.1505 Vol (1.465 < Vol < 1.474). \quad (13)$$

The measured RMS voltage signal can be converted into strain through Equation (13). The above shows that the device not only qualitatively determines the various stages of strain but also quantitatively calculates the actual strain in carbon steel based on the RMS value of the voltage.

5. Conclusions

In view of the shortcomings of current steel structures strain real-time detection methods, this paper presents a method for real-time strain detection in steel structures based on the eddy current effect and develops a relevant detection device. The device consists mainly of an eddy current probe and a signal processing system. The experimental results show that the device can not only detect the various stages of strain in Q235 steel specimens but also obtain a linear equation for the RMS voltage and the strain during the elastic phase, thus achieving the qualitative and quantitative detection of strain. The following conclusions were reached:

(1) Through theoretical analysis, this paper effectively uses the eddy current effect to convert the change of conductivity and permeability caused by steel structure strain into electrical signals, then the change rule of RMS voltage is used to characterize the state of strain.. This method can not only quantitatively detect the strain in the elastic range but also dynamically analyze different strain stages

(2) This system can complete the conversion of multiple detection modes, such as coupled array sensing detection, automatic scanning, and handheld. At the same time, the automatic frequency selection function can be completed according to different detection objects to obtain the best skin depth. According to different application scenarios and tested objects, different detection modes and excitation frequencies can be used to obtain the best detection effect. In this paper, the experiment adopts the coupling detection mode, and the data shows that the system can acutely detect dynamic strain in real time

(3) In the face of steel structures with different Young's modulus in the application field, it is only necessary to conduct tensile tests on the materials in advance to obtain the required characteristic parameters of the system, and then this method can be used to accurately convert the RMS voltage collected in the field into the stress and strain state. This shows that this method is universal and can adapt to complex practical applications

The device has the characteristics of fast, high sensitivity and real-time online monitoring. It can effectively prevent the failure of the steel structures caused by excessive strain to avoid dangerous accidents of special equipment and protect the safety of people's lives and properties.

Data Availability

The data used to support the findings of this study are available from the corresponding author upon request.

Conflicts of Interest

The authors declare no conflicts of interest.

Acknowledgments

This study was funded by the Key Research and Development Program of Zhejiang Province"development and application of key technologies for safety early warning and prevention and control of large amusement facilities" (Grant no. 2019C03114).

References

[1] Y. Zhang, P. Y. Qin, W. M. Lin, and Y. Xiao, "Research on operating condition testing syst key technologies for large amusement rides," *Chinese Journal of Safety Science*, vol. 18, no. 12, 2008.

[2] G. T. Shen, Y. Liu, J. J. Zhang, and B. Hu, "Research on health evaluation method of large amusement facilities in service," *Journal of Mechanical Engineering*, vol. 56, no. 10, pp. 1–11, 2020.

[3] D. H. Chen, "Application and development of nondestructive testing technology in special equipment manufacturing," *Modern Manufacturing Technology and Equipment*, vol. 57, no. 2, pp. 138-139, 2021.

[4] X. Liu, *Design and experiment of multifunction eddy current testing system, [Ph.D. thesis]*, Tianjin University, 2014.

[5] T. Matsumoto, T. Uchimoto, T. Takagi et al., "Investigation of electromagnetic nondestructive evaluation of residual strain in low carbon steels using the eddy current magnetic signature (EC-MS) method," *Journal of Magnetism and Magnetic Materials*, vol. 479, pp. 212–221, 2019.

[6] Z. X. Fu, "Basis of eddy current method for stress and strain detection," *Experimental Mechanics*, vol. 6, no. 2, pp. 227–232, 1991.

[7] W. N. Hou, *Study on the Influence of Stress on Defects and Detection of Ferromagnetic Materials, [Ph.D. thesis]*, China University of Petroleum (East China), 2003.

[8] T. Szumiata, K. Hibner, K. Dziewiecki et al., "Stress monitoring in steel elements via detection of AC magnetic permeability changes," *Acta Physica Polonica A*, vol. 133, no. 3, pp. 719–721, 2018.

[9] P. Bai, P. Shi, Y. Zhao, H. E. Chen, S. Xie, and Z. Chen, "Joint effect of residual stress and plastic deformation on pulsed eddy current response signals in 304 austenitic stainless steel," *International Journal of Applied Electromagnetics and Mechanics*, vol. 63, no. 1, pp. 19–30, 2020.

[10] T. Xu, *Research on bridge eddy current testing system based on impedance analysis, [Ph.D. thesis]*, North University of China., 2009.

[11] N. Zhang, C. Ye, L. Peng, and Y. Tao, "Eddy current probe with three-phase excitation and integrated array TMR sensors," *IEEE Transactions on Industrial Electronics*, vol. 68, no. 6, pp. 5325–5336, 2020.

[12] B. Liu, *Development of Special Eddy Current Testing Transducer, [Ph.D. thesis]*, China Academy of Engineering Physics, 2006.

[13] M. C. Wen and P. Xia, *Mechanics of Materials*, Tsinghua University Press, Beijing, China, 2019.

[14] J. L. Ren, J. M. Lin, and K. B. Xu, *Eddy Current Testing*, China Machine Press, Beijing, China, 2013.

[15] M. M. Yue, *Research on Detection Mechanism and Application of Differential Coil Eddy Current Sensor, [Ph.D. thesis]*, Beijing Institute of Technology, 2018.

[16] X. E. Liu, G. L. Niu, X. Y. Sun, X. C. Li, and Y. Q. Wang, "Research and design of electromagnetic nondestructive testing circuit system," *Electronic Production*, vol. 4, no. 1, 2021.

[17] F. A. Nunez-Moreno and J. D. Tole-Lozano, "Correlation study between the surface-magnetic response and sinusoidal axial-tensile strain on a butt-weld connection performed on ASTM A36 steel," *Journal of Materials in Civil Engineering*, vol. 32, no. 8, article 04020204, 2020.

[18] Y. K. Wang and J. X. Zhao, "Tensile fracture test and numerical simulation of steel," *Journal of Plastic Engineering*, vol. 26, no. 1, pp. 168–173, 2019.

[19] B. Cao, T. Iwamoto, and P. P. Bhattacharjee, "An experimental study on strain-induced martensitic transformation behavior in SUS304 austenitic stainless steel during higher strain rate deformation by continuous evaluation of relative magnetic permeability," *Materials Science and Engineering: A*, vol. 774, article 138927, 2020.

[20] W. Tang, L. Zhang, S. E. Zhou, and T. Chen, "Application of joint digital filtering in eddy current testing data acquisition system," *Journal of Jiangsu University of Science and Technology (Natural Science Edition)*, vol. 25, no. 3, 2011.